

FIG. 1. (Color online) For unstrained  $\text{Fe}_2\text{I}_2\text{Br}$  monolayer, the element (Fe, Br and I) character of the spin-up (Left) and spin-down (Right) using GGA.

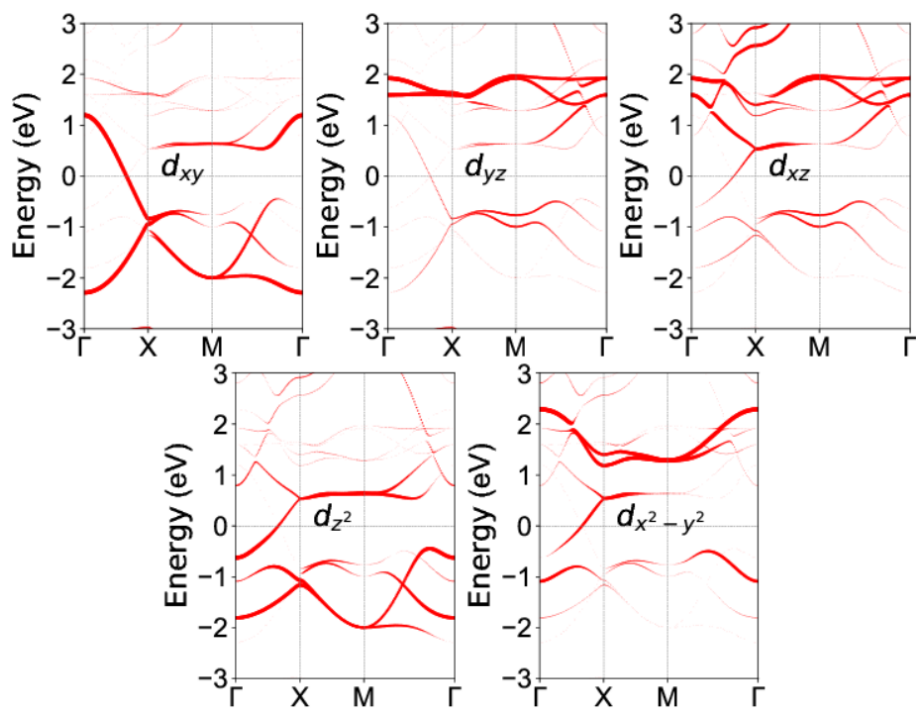


FIG. 2. (Color online) For unstrained  $\text{Fe}_2\text{I}_2\text{Br}$  monolayer, the  $d$ -orbital character of the minority-spin bands for Fe using GGA.

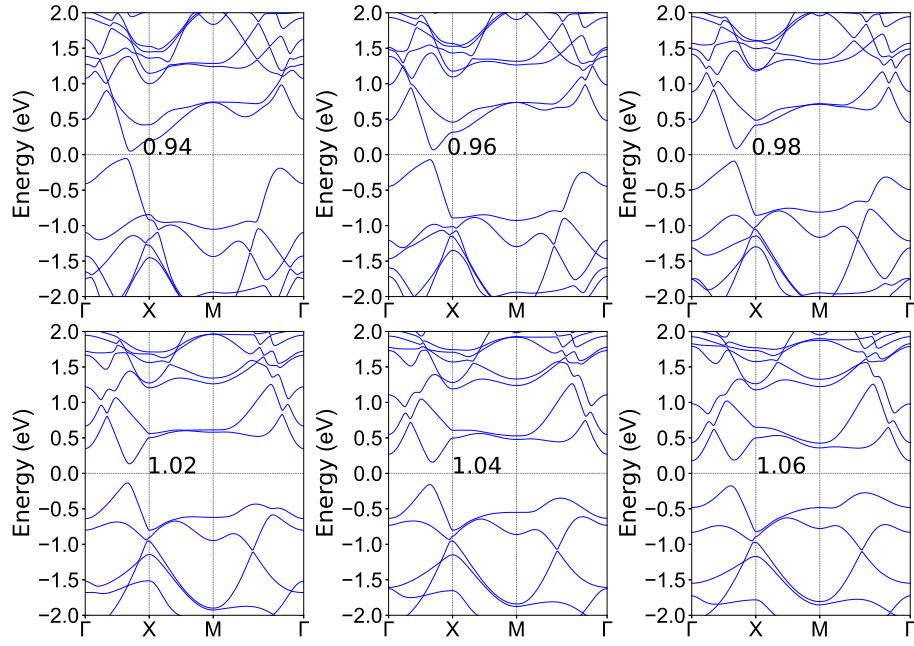


FIG. 3. (Color online) The energy band structures of  $\text{Fe}_2\text{I}_2\text{Cl}$  monolayer using GGA+SOC with  $a/a_0$  changing from 0.94 to 1.06.

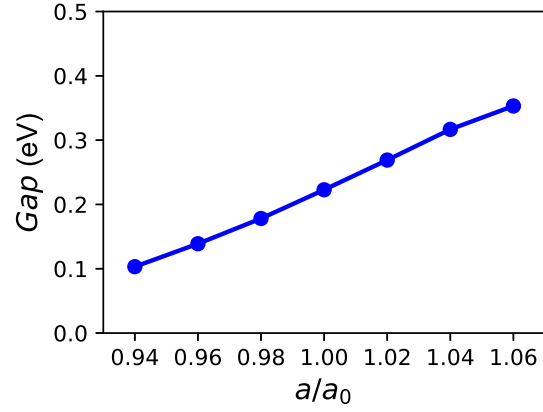


FIG. 4. (Color online) For monolayer  $\text{Fe}_2\text{I}_2\text{Cl}$ , the gap with the application of biaxial strain (0.94 to 1.06) using GGA+SOC.

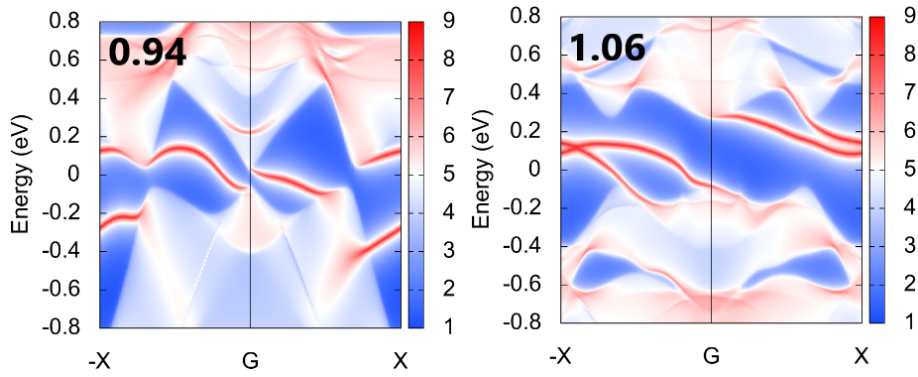


FIG. 5. (Color online) Topological edge states of  $\text{Fe}_2\text{I}_2\text{Cl}$  calculated along the (100) direction at 0.94 and 1.06 strains.

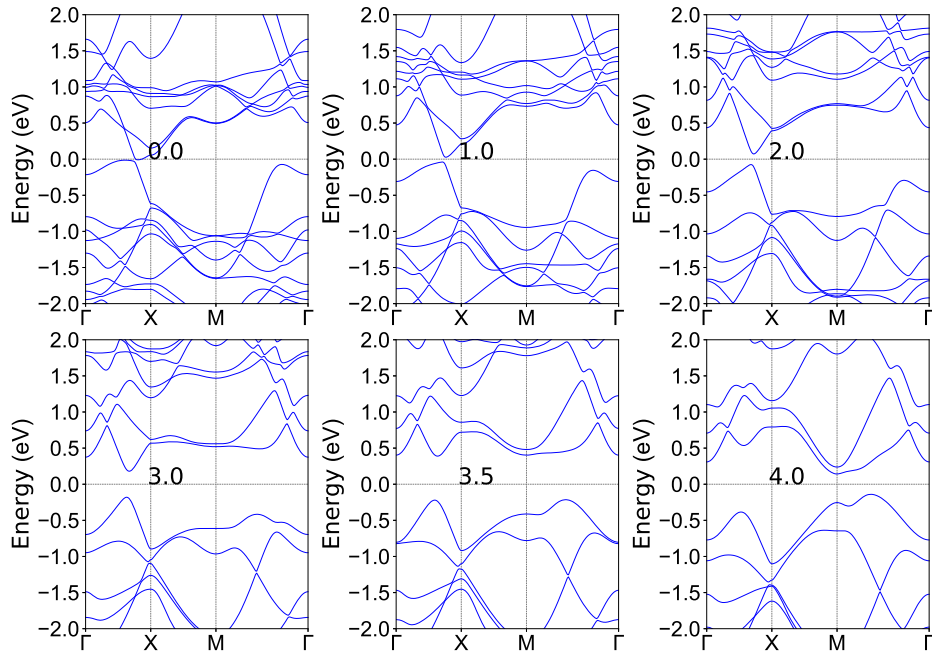


FIG. 6. (Color online) The energy band structures of Fe<sub>2</sub>ICl monolayer using GGA+SOC with six different  $U$  values (0.0, 1.0, 2.0, 3.0, 3.5 and 4.0 eV).

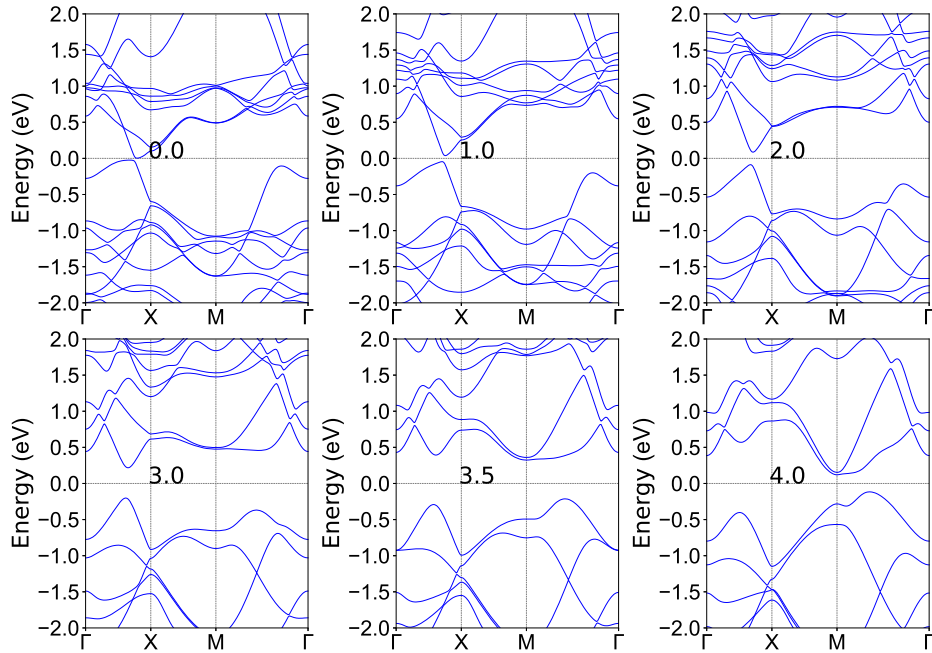


FIG. 7. (Color online) The energy band structures of Fe<sub>2</sub>IBr monolayer using GGA+SOC with six different  $U$  values (0.0, 1.0, 2.0, 3.0, 3.5 and 4.0 eV).

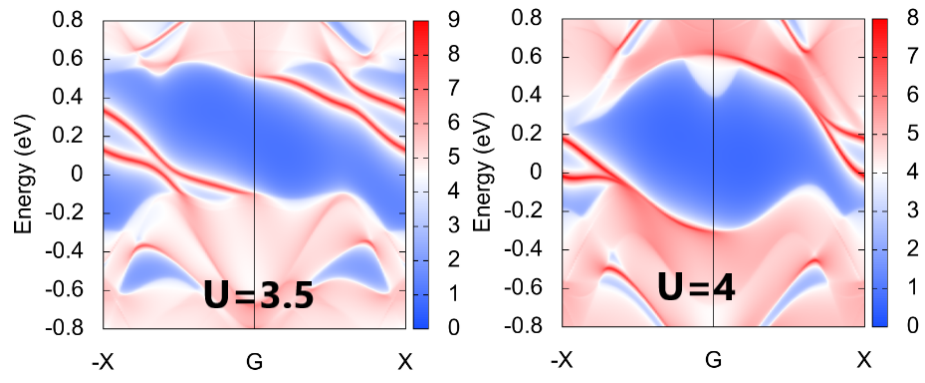


FIG. 8. (Color online) Topological edge states of  $\text{Fe}_2\text{ICl}$  calculated along the  $(100)$  direction at  $U=3.5$  eV and  $U=4.0$  eV.